PROCEEDINGS OF SCIENCE

New results on two-particle correlations in proton-proton collisions at 13 TeV from ATLAS at the LHC

Miguel Arratia* **(on behalf of the ATLAS Collaboration)**
University of Cambridge
E-mail: marratia@cern.ch

ATLAS measurements of two-particle correlations in $\sqrt{s}$ = 13 TeV pp collisions at the LHC are summarized. In high-multiplicity events, long-range rapidity correlation of particles with small azimuthal separation, i.e the "ridge", is observed with features similar to those seen in measurements of Pb+Pb, p+Pb, and lower-energy pp collisions. These results are compatible, within uncertainties, with CMS 7 TeV pp measurements.

The European Physical Society Conference on High Energy Physics
22–29 July 2015
Vienna, Austria

*Speaker.

PoS(EPS-HEP2015)211

1. Introduction

Studies of two-particle correlations in high-multiplicity pp collisions revealed features that are uncannily similar to those observed in heavy-ion collisions [1]. The number of charged-particle pairs produced with small azimuthal-angle separation is enhanced over a wide range of pseudorapidity differences. The cause of this novel phenomenon, known as the "ridge", remains unknown.

This document summarizes the ATLAS measurement of two-charged-particle correlations in 13 TeV pp collisions at the LHC [2]. This analysis uses 14 nb^{-1} collected during a low-luminosity run (average number of interactions per beam crossing 0.002–0.04) that took place in June 2015.

2. ATLAS detector, efficiencies

Reference [3] describes the ATLAS[1] detector in detail. This measurement used the ATLAS inner detector (ID), minimum-bias trigger scintillators (MBTS), and the trigger and data acquisition systems. The Level-1 trigger (MinBias) requires a signal in at least one MBTS counter; a high-multiplicity trigger (HMT) requires a signal in at least one counter on each side of the MBTS, at least 900 hits in the silicon strip tracker, and at least 60 tracks with $p_{\mathrm{T}} > 0.4$ GeV.

This analysis uses tracks with $p_{\mathrm{T}} > 0.3$ GeV and $|\eta| < 2.5$, reconstructed in the ID and selected as described in Ref. [2]. The pp events used have at least one primary vertex. For events with multiple vertices, only tracks associated with the vertex with the largest $\sum p_{\mathrm{T}}^2$ are used. Here the sum runs over the tracks associated with each vertex. The charged-particle multiplicity, $\mathrm{N}_{\mathrm{ch}}^{\mathrm{rec}}$, is defined as the number of tracks with $p_{\mathrm{T}} > 0.4$ GeV associated with the vertex with the largest $\sum p_{\mathrm{T}}^2$. Figure 1 shows the distribution of $\mathrm{N}_{\mathrm{ch}}^{\mathrm{rec}}$ and the MinBias and HMT trigger efficiencies.

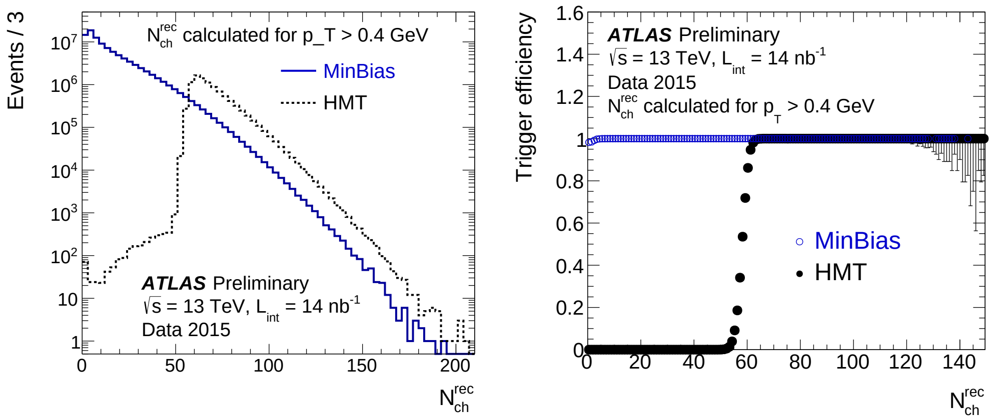

Figure 1: Left: Number of tracks with $p_{\mathrm{T}} > 0.4$ GeV, $\mathrm{N}_{\mathrm{ch}}^{\mathrm{rec}}$, in events selected by the MinBias and HMT triggers. Right: MinBias and HMT trigger efficiency as a function of $\mathrm{N}_{\mathrm{ch}}^{\mathrm{rec}}$. Figure from Ref. [2].

The MinBias trigger is fully efficient for $\mathrm{N}_{\mathrm{ch}}^{\mathrm{rec}} \geq 5$ while the HMT is 90% efficient for $\mathrm{N}_{\mathrm{ch}}^{\mathrm{rec}} \geq 60$ and fully efficient for $\mathrm{N}_{\mathrm{ch}}^{\mathrm{rec}} \geq 65$. The tracking efficiency, $\varepsilon(p_{\mathrm{T}}, \eta)$, which is evaluated using Monte

[1] ATLAS uses a right-handed coordinate system with its origin at the nominal interaction point (IP) in the center of the detector and the z-axis along the beam pipe. The x-axis points from the IP to the center of the LHC ring, and the y-axis points upward. Cylindrical coordinates (r, ϕ) are used in the transverse plane, ϕ being the azimuthal angle around the beam pipe. The pseudorapidity is defined in terms of the polar angle θ as $\eta = -\ln\tan(\theta/2)$. Transverse momentum is denoted by $\vec{p}_{\mathrm{T}}$.

Carlo simulation, increases with p_T by less than 6% between 0.3 and 0.6 GeV, and varies only weakly for $p_T > 0.6$ GeV, where it ranges from 88–90% at $\eta = 0$ to 77–80% at $|\eta| = 1.5$ and 68–73% for $|\eta| > 2.0$

3. Two-particle correlation analysis

This analysis follows methods used in previous ATLAS measurements in Pb+Pb and *p*+Pb collisions [4, 5, 6]. Two-particle correlations for charged particle pairs with transverse momenta p_T^a and p_T^b are measured as a function of $\Delta\phi = \phi^a - \phi^b$ and $\Delta\eta = \eta^a - \eta^b$, with $|\Delta\eta \leq 5|$, determined by the acceptance of the ID. The correlation function is defined as:

$$C(\Delta\eta,\Delta\phi) = \frac{S(\Delta\eta,\Delta\phi)}{B(\Delta\eta,\Delta\phi)} \tag{3.1}$$

where S and B are pair distributions constructed with pairs in the same event and in mixed events respectively. Both distributions are corrected for the tracking efficiency of the pair $\varepsilon(p_T^a,\eta^a)\varepsilon(p_T^b,\eta^b)$. Detector acceptance effects largely cancel in the ratio.

Figure 2 shows correlation functions for N_{ch}^{rec} intervals 10–30 (left) and ≤ 120 (right), for track pairs with $0.5 < p_T^a, p_T^b < 5.0$ GeV. Both correlation functions show a prominent peak at $\Delta\eta = \Delta\phi = 0$, and a $\Delta\eta$-dependent enhancement centered at $\Delta\phi = \pi$. These structures arise primarily from jets and dijets respectively. In the high-multiplicity interval, $C(\Delta\eta,\Delta\phi)$ presents a significant enhancement, or "ridge"-like structure, at $\Delta\phi = 0$ that extends over the full $\Delta\eta$ range.

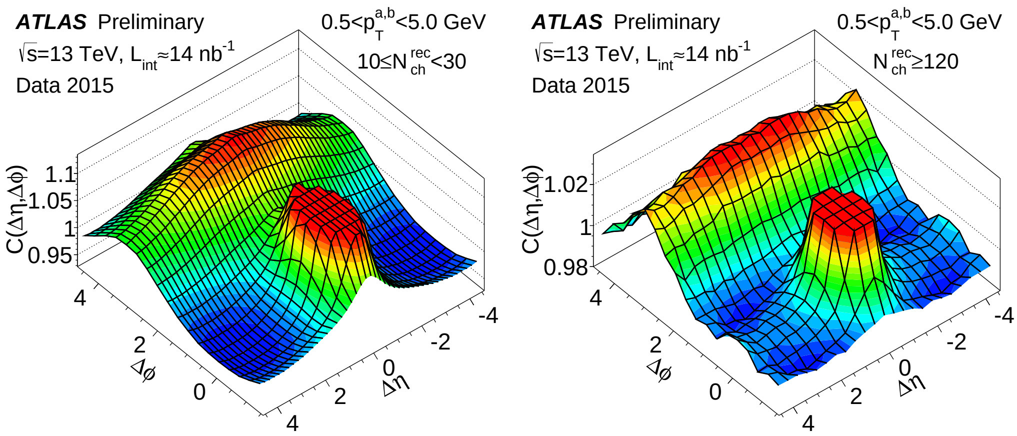

Figure 2: Two-particle correlation functions, $C(\Delta\eta,\Delta\phi)$, measured in events with low (left) and high (right) charged-particle multiplicity, N_{ch}^{rec}. The plots have been truncated to suppress the peak at $\Delta\eta = \Delta\phi = 0$. In both cases the pairs have $0.5 < p_T^{a,b} < 5.0$ GeV. Figure from Ref. [2].

To focus on the long-range features, one-dimensional correlation functions, $C(\Delta\phi)$, are obtained by integrating the numerator and denominator of Eq. 3.1 over $2 < |\Delta\eta| < 5$. Figure 3 shows the $C(\Delta\phi)$ distribution in different intervals of N_{ch}^{rec}; all four $C(\Delta\phi)$ distributions show a strong peak centred at $\Delta\phi = \pi$ that arises from the dijets. In the interval 10< N_{ch}^{rec} <30 interval, $C(\Delta\phi)$ shows a

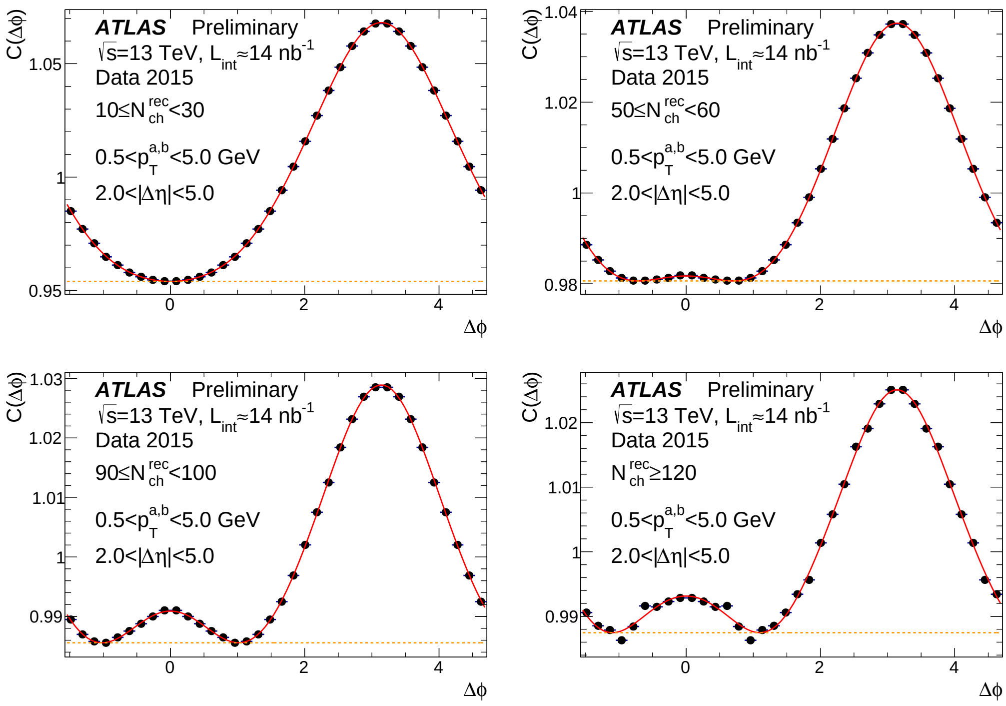

Figure 3: Two-particle correlation functions, $C(\Delta\phi)$, measured in different intervals of charged-particle multiplicity, N_{ch}^{rec}. In all cases the pairs have $0.5 < p_T^{a,b} < 5.0$ GeV, and $2 < |\Delta\eta| < 5$. The solid lines show the result of a Fourier fit to the data using harmonics up to fifth order. Figure from Ref. [2].

minimum at $\Delta\phi = 0$; with increasing N_{ch}^{rec}, this minimum fills in, and a peak appears and increases in amplitude. A Fourier series with harmonics up to fifth order fits the data well.

Figure 4 shows $C(\Delta\phi)$ measured in the $N_{ch}^{rec} > 100$ interval for two ranges of p_T^a: 0.5–1 GeV and 1–2 GeV, with p_T^b allowed to vary over 0.5–5 GeV. The amplitude of the peak at $\Delta\phi = 0$ is larger for the higher p_T^a interval.

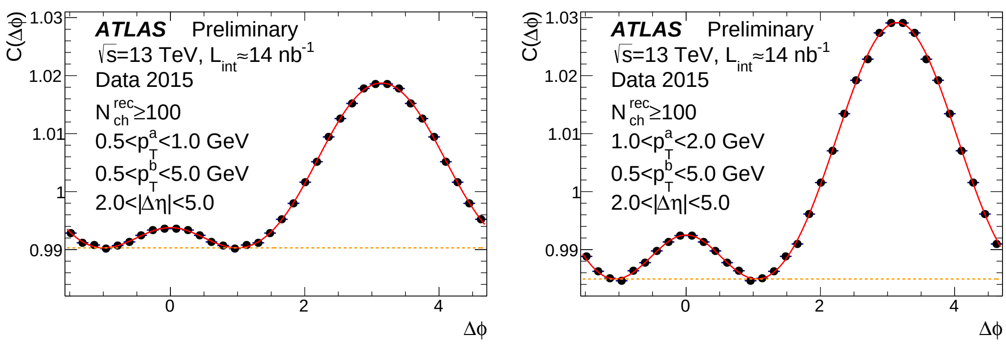

Figure 4: Two-particle correlation functions, $C(\Delta\phi)$, measured in different intervals of transverse momentum. In all cases the pairs have $2 < |\Delta\eta| < 5$. The solid lines show the result of a Fourier fit to the data using harmonics up to fifth order. Figure from Ref. [2].

Following the ZYAM method [7, 8], the effect of uncorrelated pairs on $C(\Delta\phi)$, which is estimated from the constant in the Fourier fit (see Fig. 3), is subtracted; then, the resulting function is normalized to the average number of pairs associated with each particle in the $\Delta\phi$ interval; this defines the “per-trigger-particle yield", $Y(\Delta\phi)$. The integral of the $Y(\Delta\phi)$ between the two minima near $\Delta\phi = 0$, which are obtained from the Fourier fit, defines the ridge yield, Y_{int}.

The dominant systematic uncertainties on Y_{int} arise from tracking efficiency (4%), assumptions in the ZYAM procedure (4%) and consistency of the method tested with simulation (4%).

Figure 5 shows the ridge yield as a function of charged-particle multiplicity for same-charge pairs, opposite-charge pairs, and all pairs. In all cases Y_{int} is consistent with zero for $\text{N}_{\text{ch}}^{\text{rec}} < 40$ within uncertainties, but increases linearly with $\text{N}_{\text{ch}}^{\text{rec}}$ for $\text{N}_{\text{ch}}^{\text{rec}} > 40$. The results from same-charge pairs and opposite-charge pairs are consistent within statistical uncertainties; this rules out resonances or single jets as possible sources of this phenomenom.

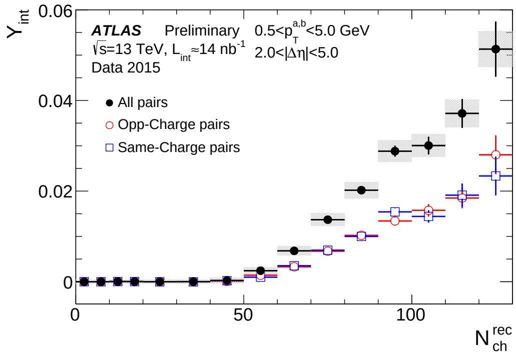

Figure 5: Ridge yield vs charged-particle multiplicity. Results are shown for all pairs, same-charge pairs and opposite-charge pairs. The error bars and shaded bands indicate statistical and systematic uncertainties (for clarity only shown in the all pairs case). Figure from Ref. [2].

Figure 5 shows Y_{int} as a function of p_{T}^{a} for $0.5 < p_{\text{T}}^{b} < 5$ GeV for three different $\text{N}_{\text{ch}}^{\text{rec}} >$ intervals; in all cases it increases up to $p_{\text{T}}^{a} < 2.5$ GeV and decreases for larger p_{T}^{a}. This behaviour is similar to p+Pb and Pb+Pb measurements [4, 5, 6].

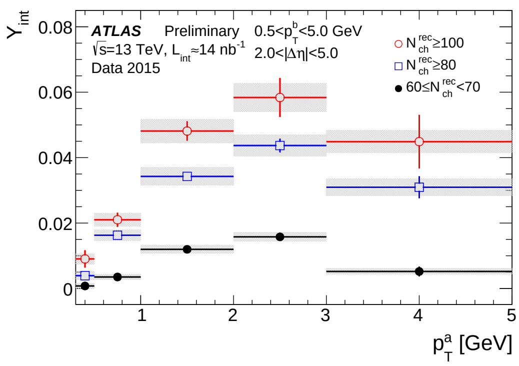

Figure 6: Ridge yield vs p_{T}^{a} measured in different $\text{N}_{\text{ch}}^{\text{rec}}$ intervals. The error bars and shaded bands indicate statistical and systematic uncertainties. Figure from Ref. [2].

Figure 7 shows a comparison of the measured Y_{int} with CMS 7 TeV pp data [1], which were obtained using similar analysis methods, as a function of $\text{N}_{\text{ch}}^{\text{rec}}$ and $p_{\text{T}}^{a,b}$. The differences in analysis

PoS(EPS-HEP2015)211

methods are taken into account, as described in Ref. [2]. The measured $Y_{\rm int}$ at 7 and 13 TeV agree within uncertainties.

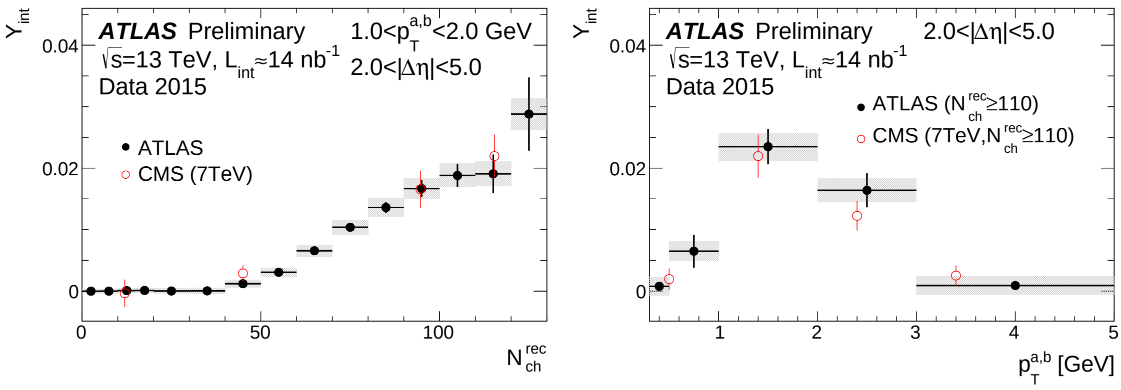

Figure 7: Comparison of the measured $Y_{\rm int}$ from this analysis to that measured by CMS at 7 TeV [1]. The ATLAS data are plotted at the centres of the corresponding $\rm N_{ch}^{rec}$ and $p_{\rm T}^{a,b}$ intervals; CMS data are plotted at the mean values. The bars and shaded bands in ATLAS data represent statistical and systematic uncertainties, respectively; the error bars in the CMS data represent the total uncertainty. Figure from Ref. [2].

4. Conclusions

Two-particle correlation functions in high-multiplicity pp collisions at $\sqrt{s} = 13$ TeV show a ridge whose strength increases with charged-particle multiplicity, and has a strong $p_{\rm T}$ dependence. These results are compatible, within uncertainties, with previous CMS 7 TeV pp measurements [1].

5. Acknowledgments

Miguel Arratia was supported by CONICYT and Cambridge Trust.

References

[1] CMS Collaboration, *Observation of Long-Range Near-Side Angular Correlations in Proton-Proton Collisions at the LHC*, JHEP **09** (2010) 091, arXiv:1009.4122 [hep-ex].

[2] ATLAS Collaboration, *Measurement of two–particle correlations in $\sqrt{s}$=13 TeV proton–proton collisions with the ATLAS detector at the LHC*, ATLAS-CONF-2015-027, http://cds.cern.ch/record/2037663.

[3] ATLAS Collaboration, *The ATLAS Experiment at the CERN Large Hadron Collider*, JINST **3** (2008) S08003.

[4] ATLAS Collaboration, *Measurement of the azimuthal anisotropy for charged particle production in $\sqrt{s_{NN}}$ = 2.76 TeV lead-lead collisions with the ATLAS detector*, Phys. Rev. **C86** (2012) 014907, arXiv:1203.3087 [hep-ex].

[5] ATLAS Collaboration, *Measurement of the distributions of event-by-event flow harmonics in lead-lead collisions at $\sqrt{s_{NN}}$= 2.76 TeV with the ATLAS detector at the LHC*, JHEP **11** (2013) 183, arXiv:1305.2942 [hep-ex].

[6] ATLAS Collaboration, *Measurement of the correlation between flow harmonics of different order in lead-lead collisions at $\sqrt{s_{NN}}$=2.76 TeV with the ATLAS detector*, Phys. Rev. **C92** (2015) 034903, arXiv:1504.01289 [hep-ex].

[7] N. N. Ajitanand et al., *Decomposition of harmonic and jet contributions to particle-pair correlations at ultra-relativistic energies*, Phys. Rev. **C72** (2005) 011902, arXiv:nucl-ex/0501025 [nucl-ex].

[8] Adare, A. et al. (PHENIX Collaboration), *Dihadron azimuthal correlations in Au+Au collisions at $\sqrt{s_{NN}}$ = 200 GeV*, Phys. Rev. **C78** (2008) 014901, arXiv:0801.4545 [nucl-ex].